International Journal of Heat and Mass Transfer 65 (2013) 713–718

Contents lists available at SciVerse ScienceDirect

International Journal of Heat and Mass Transfer

journal homepage: www.elsevier.com/locate/ijhmt

A study of near-infrared nanosecond laser ablation of silicon carbide

Doan Hong Duc *, Iwatani Naoki, Fushinobu Kazuyoshi

Tokyo Institute of Technology, Box I6-3, Meguro-ku, Tokyo 152-8550, Japan

A R T I C L E I N F O

Article history:
Received 31 July 2012
Accepted 20 June 2013
Available online 19 July 2013

Keywords:
Laser ablation
Silicon carbide
Ablation threshold
Free carrier absorption

A B S T R A C T

This work presents a fundamental study about ablation threshold, absorption coefficient and absorption mechanism of silicon carbide (SiC) in the laser drilling process. Experimental study has been performed on single infrared (1064 nm) ns pulse laser ablation of SiC at various fluence values. Hole diameters were measured to predict the absorption threshold. Based on the ablation threshold, an average absorption coefficient of SiC at infrared wavelength during the laser ablation process is calculated. The result is discussed based on absorption coefficient dependence on doping concentration and temperature in semiconductor. A preliminary model is proposed that accounts for the heat conduction and surface evaporation to predict the cross-sectional shape of drilling hole. Analytical modeling results are in good agreement with observed features produced from the laser. The paper will conclude with suggestions for further research and potential applications for the work.

1. Introduction

The success of microelectronics has been followed by rapid development in microelectro-mechanical systems (MEMS) where silicon (Si) is currently the leading material. Nowadays there is an increased demand for devices capable of functioning at high temperatures and in harsh environments, which exceed the physical properties of Si. This demand accounts for the emergence of SiC, with higher band-gap, higher breakdown threshold, higher thermal conductivity and higher saturation velocity than Si, as preferred material for MEMS in the future.

Unfortunately some of these properties of SiC are also barriers to the fabrication of microelectronics and MEMS devices. Conventional dry etching techniques of via through SiC wafers requires time-consuming mechanical thinning to a thickness of ~100 μm. Typical etch rates for 4H and 6H SiC substrates in F_2- or Cl_2-based plasmas range between 0.2 μm/min and 1.3 μm/min [1–4]. In contrast to the chemical-based micro-fabrication methods, laser ablation of SiC is capable of higher etching rates [5–7] and precise control of via size with advancement of the reduction in the number of processing steps as masking, machining independent of crystal structure, and curved surfaces. Laser ablation of SiC has been carried out with pulse durations from nanosecond to femtosecond regime. Femtosecond lasers have produced little contamination and low HAZ [8–10]. However, the lower etch rates via formation compared with nanosecond laser and the high cost of machining system still are the problem to spread out. In the practical system, the ns pulse laser machining is widely used.

Single-crystalline SiC is practically transparent at visible wavelengths, but has an optical absorption on the order of $10^5\ \mathrm{cm}^{-1}$ in the UV regime due to the intrinsic absorption of photon energy. Nanosecond pulsed UV lasers such as excimer and frequency tripled and quadrupled Nd:YAG are the most widely used [11–14] due to their prevalence and the high optical absorption of crystalline SiC at UV wavelengths. It is concluded that UV laser ablation is an effective but slow material removal process for SiC wafers compared to infrared lasers such as 1064 nm Nd:YAG [14]. Although the advantages of low cost and high speed material removal process, the important parameters such as ablation threshold, absorption coefficient for near-infrared laser ablation of SiC are still very limited. This work presents a fundamental study about near-infrared laser ablation threshold, absorption coefficient and absorption mechanism of SiC in the laser drilling process experimentally and theoretically.

2. Estimating ablation threshold and absorption coefficient

In this section, an experiment to estimate the ablation threshold and absorption coefficient of SiC is carried out. First, the method by using the diameters of drilled vias and applied energy of laser pulses [15] is discussed. Assuming that the laser pulse has a Gaussian spatial distribution:

$$F(r) = F_0 \exp\left(\frac{-2r^2}{r_0^2}\right) \tag{1}$$

$$F_0 = \frac{2E}{\pi r_0^2} \tag{2}$$

---

* Corresponding author. Tel./fax: +81 3 5734 2500.
E-mail address: doan.d.aa@m.titech.ac.jp (D.H. Duc).

0017-9310/$ - see front matter © 2013 Elsevier Ltd. All rights reserved.
http://dx.doi.org/10.1016/j.ijheatmasstransfer.2013.06.050

Nomenclature

c	speed of light, m/s
e	electron charge, C
E	pulse energy, J
f	focal length, m
F	laser fluence, J/cm^2
F_0	peak fluence at the beam center, J/cm^2
F_{th}	ablation threshold, J/cm^2
h	enthalpy per unit volume, J/m^3
H_{latent}	latent energy density, J/m^3
H_{removal}	removal energy density, J/m^3
H_{sens}	sensible energy density, J/m^3
I_0	laser intensity, W/m^2
k	thermal conductivity, W/(m K)
k_B	Boltzmann constant, J/K
L	thickness of SiC wafer, m
L_m	latent heat of melting, J/atom
L_v	latent heat of vaporization, J/atom
m^*	charge carrier effective mass, kg
N_D	impurity concentration, m^{-3}
n	refractive index of SiC
P	laser power, W
P_a	ambient pressure, Pa
r	radial distance
r_0	beam radius, m
R	reflectivity
R_v	universal gas constant, J/(mol K)
s	volumetric heat generation rate, W/m^3
t_0	pulse width, ns
T	temperature, K
T_∞	ambient temperature, K
T_m	melting temperature, K
T_c	critical temperature, K
T_s	surface temperature, K
v_s	surface velocity, m/s
z	axial distance, m
z_s	surface distance, m

Greek symbols

α	absorption coefficient, cm^{-1}
ε_0	permittivity, F/m
λ	laser beam wavelength, nm
μ	electron mobility, cm^2/(V s)
ρ	density of liquid medium, kg/m^3
ρ_l	density of liquid silicon, kg/m^3
ρ_s	density of solid SiC, kg/m^3
ω	beam waist of the laser before lens, m

Here r, F_0 and E are beam radius, peak fluence at the beam center and the pulse energy, respectively. If the laser pulse ablates the SiC only when the fluence is above the ablation threshold, the relationship between the diameters of ablation hole and the ablation threshold is following:

$$D^2 = 2r_0^2 \ln\left(\frac{F_0}{F_{\text{th}}}\right) \tag{3}$$

Here D and F_{th} are the diameter of the single shot ablated via and ablation threshold value, respectively. Substituting for the peak fluence from Eq. (2)

$$D^2 = 2r_0^2 \ln(E) - 2r_0^2 \ln\left(\frac{\pi r_0^2 F_{\text{th}}}{2}\right) \tag{4}$$

By fitting the relationship between the diameters of ablation hole and applied energy of laser pulses, the spot size of the laser pulse can be obtain from the slope of the graph of D^2 versus $\ln(E)$. Using the spot size and the intercept of the same graph, the threshold fluence can be found.

A commercial 4H–SiC wafer (10 × 10 × 0.34 mm) was used for laser drilling. The SiC sample is doped with nitrogen. The concentration of nitrogen was measured by using secondary ion mass spectrometry method as the depth-wise profile of concentration and shown in Fig. 1 with concentration of 1.8×10^{20} cm^{-3} at the surface and 1.6×10^{19} cm^{-3} in the bulk.

The infrared nanosecond laser used in this work was an Nd:YAG laser (Continuum Surelite I-10, $P = 4.72$ W, $\lambda = 1064$ nm) with the pulse duration of 6 ns. The laser is operated in the TEM$_{00}$ mode, and the laser beam profile is Gaussian, which was measured by a CCD camera. The pulse energy was controlled by an external attenuator including a variable beam splitter and a correction plate. After focused by a 10× object lens, pulse energies were measured by using a energy meter.

At each of different pulse energy level, single shot ablation experiment was carried out 5 times. The relationship between the diameters of drilled holes and applied energy of laser pulses was shown in Fig. 2. The plot points show the average experimental values. The under and upper error bars show the minimum and the maximum values of via diameter among the 5 experimental values. As shown in Fig. 2, a straight line can be fitted to represent a low energy regime and the other straight line represents a high energy regime. At low energy regime, the surface evaporation is weak, effect of plasma shielding can be ignored, and the use of Eq. (4) is acceptable. However, at high energy regime surface evaporation become stronger, effect of plasma shielding is more significant and the Eq. (4) can no longer be used. Therefore, in this experiment the results in the low energy regime are used. Estimated spot size and ablation threshold are: $r_0 = 13.6$ µm and $F_{\text{th}} = 7.8$ J/cm^2, respectively. The estimated spot size value shows a good agreement with the diffraction-limited spot size, which was calculated as

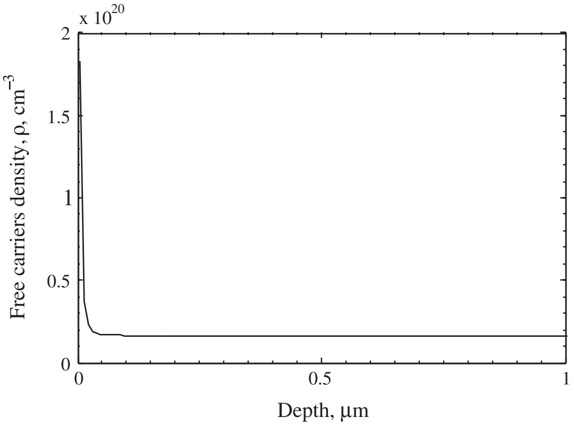

Fig. 1. Depth profile of nitrogen concentration measured by using secondary ion mass spectrometry.